phys. stat. sol. (c) **2**, No. 9, 3227–3231 (2005) / **DOI** 10.1002/pssc.200461125

Fabrication and optimization of rugate filters based on porous silicon

E. Lorenzo[1], **C. J. Oton**[*1], **N. E. Capuj**[1], **M. Ghulinyan**[2], **D. Navarro-Urrios**[2], **Z. Gaburro**[2], and **L. Pavesi**[2]

[1] Departamento de Física Básica, University of La Laguna, Avda. Astrofísico Fco. Sánchez, 38204, La Laguna, Tenerife, Spain
[2] INFM and Dipartimento di Fisica, Unversity of Trento, Via Sommarive 14, 38050 Povo (TN), Italy

Received 7 June 2004, revised 18 September 2004, accepted 27 January 2005
Published online 9 June 2005

PACS 42.79.Ci, 42.82.–m, 61.43.Gt, 68.65.Ac, 81.05.Rm

We report an experimental study of porous silicon-based rugate filters. Possible optimisations that can improve different features of the filters are investigated. We demonstrate sidelobe attenuation by means of half-apodization of the structures with a sinusoidal window. Reduction of interference ripples are experimentally observed through the insertion of index-matching layers on the boundaries of the structure. The superposition of two different designs to obtain a multi-stop-band filter is also demonstrated. We show the possibility of controlling the bandwidth of the stop-bands by varying the index contrast. All the results are discussed and compared with numerical calculations.

1 Introduction

Porous silicon (PS) has attracted the attention of material research during the last decade, after the observation of efficient visible luminescence [1]. However, PS also presents very interesting optical passive properties. Different orientations and sizes of the pores can determine very different optical properties, thus offering a wide range of applications in many fields, from optical devices to chemical and biological sensors [2].

PS shows optical properties typical of a dielectric material with an effective refractive index, n, which can be anisotropic [3]. The value of n depends directly on porosity (volumetric fraction of air). PS obtained through electrochemical etching offers the opportunity to modulate the porosity in depth since the already etched part of the layer is unaffected by subsequent current changes. This allows the fabrication of structures with any refractive index profile. In this way, one dimensional (1D) photonic structures can be grown very easily and with no need for expensive equipment. Bragg reflectors [4], microcavities [5], waveguides [6], and more complex structures [7, 8] based on PS have been realised.

All these optical structures are fabricated by just alternating the etch current between two different values: a high and a low current, which leads to low and high refractive indices, respectively. If the current is gradually modulated, a smooth index profile can be achieved, giving rise to the so-called *rugate filters*. These structures have been theoretically investigated for the last 20 years.

The possibility of gradually varying the refractive index profile can improve many different spectral features [9–11]. (i) Rugate filters do not show higher harmonics, *i.e.* reflection bands located at integer divisors of the central wavelength; (ii) if the index contrast of these structures is modulated with a

[*] Corresponding author: e-mail: cjoton@ull.es, Phone: +34 922 319872.

smooth function, the sidelobes of the reflection band are suppressed. This is called *apodization* of the index profile; (iii) the first and last interfaces of the structures can lead to reflections that produce interference ripples outside the reflection band. These ripples can be attenuated by adding *index-matching* layers on the boundaries, whose refractive index varies gradually to avoid an abrupt index change. These layers behave as broad-band antireflection coatings; (iv) rugate filters allow combining different designs by superposing their profiles in order to attain a response which is, to first approximation, the sum of the single designs.

In spite of all the advantages that rugate filters can offer, only a few experimental work have been reported, due to the limitations of the available techniques for producing and controlling continuous refractive index variations. Rugate filters made by evaporation [12, 13], reactive sputtering [14], plasma-enhanced chemical vapor deposition [15] and glancing angle deposition [16], have been reported. Glazing evaporation of silicon also allows smooth variation of refractive index [17]. The first PS-based rugate filter was reported in 1997 by Berger and coworkers [18], and in 2002, Cunin *et al*. showed an application for biomolecular screening [19]. To the best of our knowledge, these are the only works which report rugate filters based on electrochemically grown PS.

In this work we study PS-based rugate filters, in which different kinds of structures are fabricated, characterized and compared. We discuss the experimental results and compare with numerical calculations. A more detailed work will be published elsewhere [20].

2 Experiment

In this work we used p^+-type (100)-oriented silicon wafers (ρ = 0.01 Ωcm); the electrolyte was made with a 31% volumetric fraction of aqueous (48 wt.%) HF in ethanol, and the free area of the teflon mask was 1 cm^2. A platinum electrode was immersed into the electrolyte, and silicon was anodized using a computer-controlled source Agilent 6612C in current source mode. In order to detach PS from the substrate and produce freestanding samples a high current step (450 mA/cm^2 for 0.5 s) was applied at the end of the process. We employed a mechanical stirrer to keep good electrolyte exchange during anodization.

We first calibrated the optical parameters of several monolayers versus current density in a range between 2 and 110 mA/cm^2. Scanning electron microscopy and reflectance spectra allowed to determine the thickness and optical path of each sample, from which we calculated the etch rates and refractive index. Once both curves were fitted with smooth functions, any refractive index profile was attainable by controlling the current source with a computer. The index range achievable was between 1.17 and 2.42, but very low indices yield very fragile layers, and very high indices require very long times, due to the low etch rate at low currents. This limited the practical index range between 1.36 (80 mA/cm^2) and 2.25 (10 mA/cm^2). Currents outside these two values were only applied exceptionally, for instance, in index-matching layers.

The optical characterization of PS filters was carried out in a Varian Cary-5 UV-VIS-NIR spectrophotometer, with halogen VIS-NIR lamp source. A collimated beam spot size of 1 mm illuminated normally the sample, and transmission spectra were obtained in a wide wavelength range (400–2500 nm). The overall wavelength resolution of the system was 2 nm. However, an increase of the spot size until 5 mm did not yield significant changes. The aging of the samples was also characterized, a 2% blueshift was observed after 3 months since the fabrication day, as a consequence of partial oxidation of silicon. The filters presented here were designed for the near infrared region (between 1 and 2 μm). This region is important for telecommunications and for astrophysics [21], and the performance of PS-based structures are expected to be better than in the visible range, where light absorption and scattering becomes considerable.

3 Results and discussion

Figure 1 shows the transmittance spectra of four different samples. The nominal index profile is shown on the top row. The middle row shows the calculation of the transmittance spectrum from the nominal curve. The calculation is based on the transfer-matrix method, typically used for multilayers. The gradual refractive index variations were treated as discrete layers, so each oscillation was meshed into a certain number of layers until the result was independent of this number. For the sake of clarity, we considered neither silicon absorption (real index) nor dispersion (index independent of wavelength). The bottom row shows the measured transmittance spectrum.

The first column (Fig. 1A) shows a 20-period rugate filter with indices limited between 1.36 and 2.25 and centred at 1600 nm. A stop-band without higher harmonics is expected, as shown in the calculation. The experiment also shows the main stop-band, slightly narrower than expected, and a weak second harmonic. These discrepancies are due to small imperfections in the calibration curve, because it has been obtained from monolayers, and the parameters can vary slightly when porosity is modulated. The transmission decay observed below 800 nm is due to PS absorption, not considered in the calculation. In spite of these small imperfections, the agreement found between the experiment and calculations demonstrates the control on the etching process. The second column (fig. 1B) is the same design as column A but with a sinusoidal half-apodization of the index contrast [22]. As one can appreciate in the calculation and experiment, the sidelobes are suppressed, as expected. However, interference ripples still remain due to the abrupt index change at the boundaries. The signal oscillates between 100% and 90% transmittance.

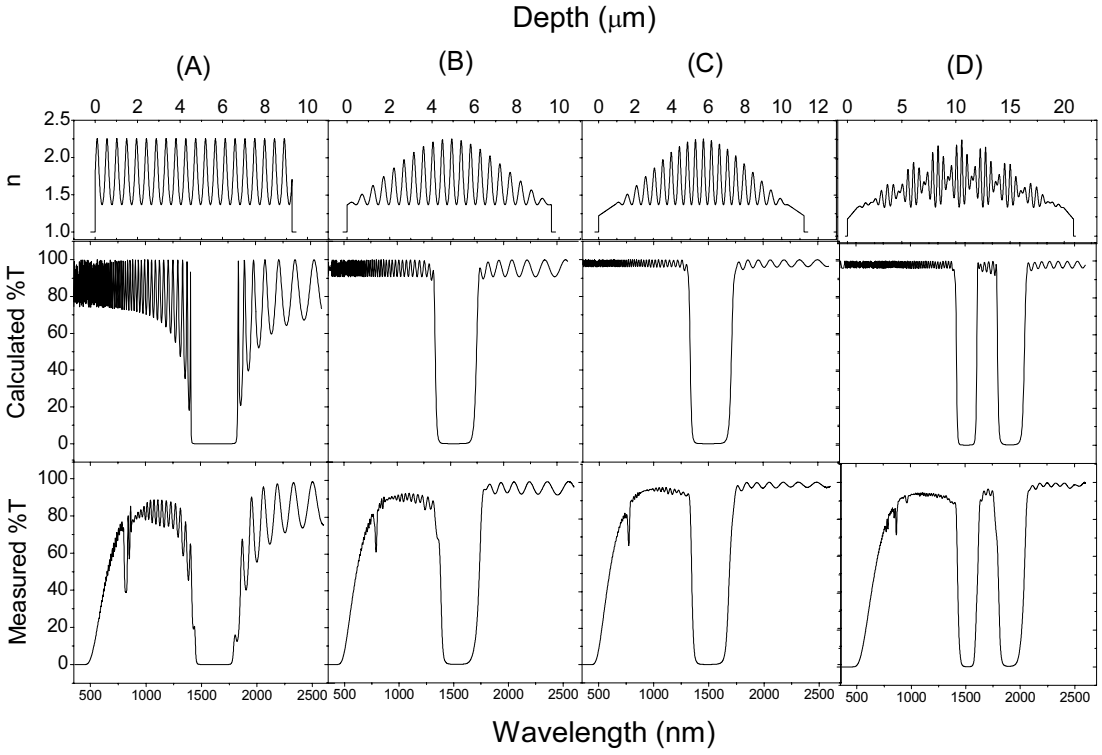

Fig. 1 The four columns represent four different samples: (A) a 20-period pure rugate; (B) same as A with a sinusoidal apodization; (C) same as B with index-matching layers; (D) sum of 40- and 32-period rugates centred at 1500 and 1900 nm, respectively, with apodization and index-matching layers. The top row shows the nominal index profile. The middle row shows the calculated transmittance of the design assuming non-dispersive (constant in energy) and real (non-absorbing) refractive indices. The bottom row shows the measured transmittance.

The third column (Fig. 1C) shows a sample made with the same design as before but with additional *index-matching* layers at the boundaries to prevent the interference ripples. As the sample is freestanding, both interfaces are with air, so the index matching layer must arrive at the lowest attainable index. In this sample, the index was varied from 1.22 to 1.36, and the intensity of the interference ripples is reduced from 10% to 5%, as expected from the calculations.

The fourth column (Fig. 1D) is a design of a double stop-band filter. Two different rugate filter designs were combined by summing two frequencies. The bands are centred at 1500 and 1900 nm and they have 40 and 32 periods, respectively. The resulting oscillating function was apodized and index-matched in the same way as the previous samples. A double stop-band is observed, with neither sidelobes nor ripples. The agreement between calculation and experiment confirms the possibility of combining different designs for creating multi-stop-band filters that block any desired wavelength band.

The optical densities (absolute value of the decimal logarithm of the transmittance) of these four filters in the middle of the stop-band are A: 3.4, B: 3.0, C: 3.0, D: 3.0 at 1500 nm and 2.48 at 1900 nm. The reason for having higher reflectance in sample A is the lack of apodization. In sample D, the difference in optical density between both stop-bands is caused by the different number of periods.

Figure 2 compares two apodized rugate filters with different index contrast. Figure 2a shows the profile of a 20-period sample contrasted between 1.36 and 2.25, and Fig. 2b, the profile of a 40-period sample contrasted between 1.36 and 1.7. The lower-contrast sample was designed with more periods because otherwise the quality of the stop-band would have decayed too much. Both samples are freestanding and index-matched to air. It is well known that the width of a stop-band is given by the index contrast of the structure. We can observe this effect in Fig. 2c in which both experimental spectra are shown. The bandwidth of the high-contrast sample is 350 nm, while for the low-contrast sample, the bandwidth decreases to 150 nm. However, the optical density of the narrow band is less than for the wide one (2.0 instead of 3.0). This example demonstrates the possibility of controlling the bandwidth of stop-band filters by varying the contrast.

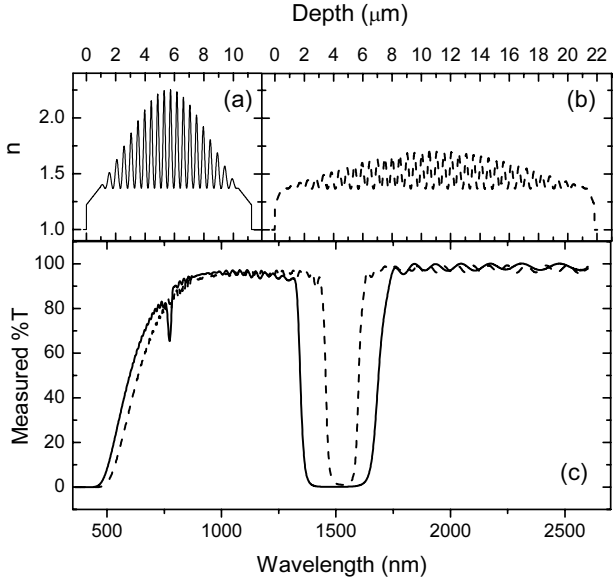

Fig. 2 Comparison between rugate filters made with different index contrast. (a) Nominal profile of a 20-period sample with 1.36–2.25 contrast, (b) 40-period sample with 1.36–1.7 contrast. (c) Transmission spectra of the high-contrast sample (solid line) and low-contrast sample (dashed line).

4 Conclusions

In this work we experimentally study porous silicon-based rugate filters. Half-apodization of rugate filters produces attenuation of sidelobes. Interference ripples are attenuated with the insertion of index-matching layers on the boundaries of the structure. We show an example of a parallel combination of two different designs, through the fabrication of a multi-stop band filter. We finally study the effect of varying the index contrast of rugate filters, in which bandwidth variations are observed. The easy and cheap procedures involved in the fabrication process make these results very attractive for applications in many fields, such as telecommunications, chemical or biological sensors and astrophysics.

Acknowledgements We thank Instituto de Astrofísica de Canarias for offering their facilities and help for the optical characterization. We acknowledge Science and Technology Ministry of Spain Project MAT 2002-00044 for financial support. C. O. acknowledges a fellowship granted by Cajacanarias and University of La Laguna.

References

[1] L. T. Canham, Appl. Phys. Lett. **57**, 1046 (1990).
[2] Properties of Porous Silicon, ed. L. T. Canham (IEE Inspec, London, U.K., 1997).
[3] C. J. Oton, M. Ghulinyan, Z. Gaburro, P. Bettotti, L. Pavesi, L. Pancheri, S. Gialanella, and N. E. Capuj, J. Appl. Phys. **94** (10), 6334 (2003).
[4] V. Agarwal and J. A. del Rio, Appl. Phys. Lett. **82**,1512 (2003).
[5] M. Ghulinyan, C. J. Oton, G. Bonetti, Z. Gaburro, and L. Pavesi, J. Appl. Phys. **93** (12), 9724 (2003).
[6] P. Ferrand, R. Romestain, and J. C. Vial, Phys. Rev. B **63**, 115106 (2001).
[7] L. Dal Negro, C. J. Oton, Z. Gaburro, L. Pavesi, P. Johnson, A. Lagendijk, R. Righini, M. Colocci, and D. S. Wiersma, Phys. Rev. Lett. **90** (5), 055501 (2003).
[8] R. Sapienza, P. Costantino, D. Wiersma, M. Ghulinyan, C. J. Oton, and L. Pavesi, Phys. Rev. Lett. **91**, 263902 (2003).
[9] B. G. Bovard, Appl. Opt. **32** (28), 5427 (1993).
[10] W. H. Southwell, Appl. Opt. **28** (23), 5091 (1989).
[11] W. H. Southwell, Appl. Opt. **36** (1), 314 (1997).
[12] C. S. Bartholomew, M. D. Morrow, H. T. Betz, J. L. Grieser, R. A. Spence, and N. P. Murarka, J. Vac. Sci. Technol. A **6**, 1703 (1988).
[13] W. J. Gunning, R. L. Hall, F. J. Woodberry, W. H. Southwell, and N. S. Gluck, Appl. Opt. **28** (14), 2945 (1989).
[14] A. F. Jankowski, L. R. Schrawyer, and P. L. Perrym J. Vac. Sci. Technol. A **9**, 1184 (1991).
[15] P. L. Swart, P. V. Bulkin, and B. M. Lacquet, Opt. Eng. **36** (4), 1214 (1997).
[16] Kate Kaminska, Tim Brown, Gisia Beydaghyan, and Kevin Robbie, Proc. SPIE Int. Soc. Opt. Eng. **4833**, 633 (2003)
[17] K. Kaminska, T. Brown, G. Beydaghyan, and Kevin Robbie, Appl. Opt. **42** (20), 4212 (2003).
[18] M. G. Berger, R. Arens-Fischer, M. Thönissen, M. Krüger, S. Billat, H. Lüth, S. Hilbrich, W. Theiss, and P. Grosse, Thin Solid Films **297**, 237 (1997).
[19] F. Cunin, T. A. Schmedake, J. R. Link, Y. Li, J. Koh, S. Bhatia, and M. Sailor, Nature Mater. **1**, 39 (2002).
[20] E. Lorenzo, C. J. Oton, N. E. Capuj et al., submitted to J. Appl. Phys.
[21] A. R. Offer and J. Bland-Hawthorn, Mon. Not. R. Astron. Soc. **299** (1), 176 (1998).
[22] H. A. Abu-Safia, A. I. Al-Sharif, and I. O. Abu Aljarayesh, Appl. Opt. **32** (25), 4831 (1993).